

Tuning the Conductance of Dirac Fermions on the Surface of a Topological Insulator

S. Mondal,¹ D. Sen,² K. Sengupta,¹ and R. Shankar³

¹Theoretical Physics Division, Indian Association for the Cultivation of Sciences, Kolkata 700 032, India

²Center for High Energy Physics, Indian Institute of Science, Bangalore 560 012, India

³The Institute of Mathematical Sciences, C.I.T Campus, Chennai 600 113, India

(Received 24 August 2009; published 29 January 2010)

We study the transport properties of the Dirac fermions with a Fermi velocity v_F on the surface of a topological insulator across a ferromagnetic strip providing an exchange field \mathcal{J} over a region of width d . We show that the conductance of such a junction, in the clean limit and at low temperature, changes from oscillatory to a monotonically decreasing function of d beyond a critical \mathcal{J} . This leads to the possible realization of a magnetic switch using these junctions. We also study the conductance of these Dirac fermions across a potential barrier of width d and potential V_0 in the presence of such a ferromagnetic strip and show that beyond a critical \mathcal{J} , the criteria of conductance maxima changes from $\chi = eV_0d/\hbar v_F = n\pi$ to $\chi = (n + 1/2)\pi$ for integer n . We point out that these novel phenomena have no analogs in graphene and suggest experiments which can probe them.

DOI: 10.1103/PhysRevLett.104.046403

PACS numbers: 71.10.Pm, 73.20.-r

The properties of topological insulators with time-reversal symmetry in both two and three dimensions (2D and 3D) have attracted a lot of theoretical and experimental attention in recent years [1–8]. Such 3D insulators can be completely characterized by four integers ν_0 and $\nu_{1,2,3}$ [4]. The former specifies the class of topological insulators to be strong ($\nu_0 = 1$) or weak ($\nu_0 = 0$), while the latter integers characterize the time-reversal invariant momenta of the system given by $\vec{M}_0 = (\nu_1\vec{b}_1, \nu_2\vec{b}_2, \nu_3\vec{b}_3)/2$, where $\vec{b}_{1,2,3}$ are the reciprocal lattice vectors. The topological features of strong topological insulators (STI) are robust against the presence of time-reversal invariant perturbations such as disorder or lattice imperfections. It has been theoretically predicted [1,4] and experimentally verified [2] that the surface of a STI has an odd number of Dirac cones whose positions are determined by the projection of \vec{M}_0 on to the surface Brillouin zone. The position and number of these cones depend on both the nature of the surface concerned and the integers $\nu_{1,2,3}$. For several compounds such as HgTe and Bi₂Se₃, specific surfaces with a single Dirac cone near the Γ point of the 2D Brillouin zone have been found [2,6,8]. Such a Dirac cone is described by the Hamiltonian

$$H = \int \frac{dk_x dk_y}{(2\pi)^2} \psi^\dagger(\vec{k}) (\hbar v_F \vec{\sigma} \cdot \vec{k} - \mu I) \psi(\vec{k}), \quad (1)$$

where $\vec{\sigma}(I)$ denotes the Pauli (identity) matrices in spin space, $\psi = (\psi_\uparrow, \psi_\downarrow)^T$ is the annihilation operator for the Dirac spinor, v_F is the Fermi velocity, and μ is the chemical potential [9]. Recently, several novel features of these surface Dirac electrons such as the existence of Majorana fermions in the presence of a magnet-superconductor interface on the surface [9,10], generation of a state resembling a $p_x + ip_y$ -wave superconductor but with time-reversal symmetry via proximity to a s -wave superconductor [9],

anomalous magnetoresistance of ferromagnet-ferromagnet junctions [11], and novel spin textures with chiral properties [8] have been studied in detail.

In this Letter, we study the transport properties of these surface Dirac fermions in two experimentally realizable situations shown in Fig. 1. The first study concerns their transport across a region with a width d with a proximity-induced exchange field \mathcal{J} arising from the magnetization $\vec{m} = m_0\hat{y}$ of a proximate ferromagnetic film as shown in the left panel of Fig. 1. We demonstrate that the tunneling conductance G of these Dirac fermions through such a junction can either be an oscillatory or a monotonically decaying function of the junction width d . One can interpolate between these two qualitatively different behaviors of G by changing m_0 (and thus \mathcal{J}) by an applied in-plane magnetic field leading to the possible use of this junction as a magnetic switch. The second study concerns the transport properties of Dirac fermions across a barrier characterized by a width d and a potential V_0 in region II with a magnetic film proximate to region III as shown in the right panel of

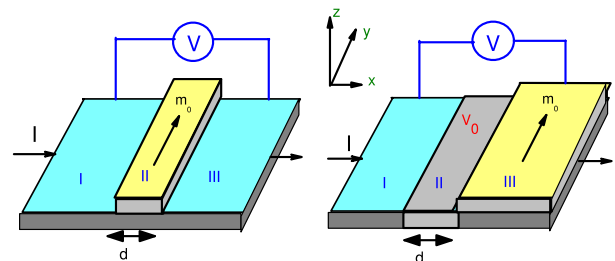


FIG. 1 (color online). Proposed experimental setups: Left panel: The ferromagnetic film extends over region II of width d providing an exchange field in this region. Right panel: The film extends over region III while the region II has a barrier characterized by a voltage V_0 . V and I denote the bias voltage and current across the junction, respectively. See text for details.

Fig. 1. We note that it is well known from the context of Dirac fermions in graphene [12] that such a junction, in the absence of the induced magnetization, exhibits transmission resonances with maxima of transmission at $\chi = eV_0d/\hbar v_F = n\pi$, where n is an integer. Here we show that beyond a critical strength of m_0 , the maxima of the transmission shifts to $\chi = (n + 1/2)\pi$. Upon further increasing m_0 , one can reach a regime where the conductance across the junctions vanishes. In this study, we restrict ourselves to the weak disorder or the clean limit and low temperature so that the mean-free path and phase coherence length for the Dirac electrons are sufficiently large. We stress that the properties of Dirac fermions elucidated here are a consequence of their spinor structure in physical spin space, and thus have no analogs for either conventional Schrödinger electrons in 2D or Dirac electrons in graphene [13–15].

We begin with an analysis of the junction shown in the left panel of Fig. 1. The Dirac fermions in regions I and III are described by the Hamiltonian in Eq. (1). Consequently, the wave functions of these fermions moving along $\pm x$ in these regions for a fixed transverse momentum k_y and energy ϵ can be written as $\psi_j^\pm = (1, \pm e^{\pm i\alpha}) \exp(i(\pm k_x x + k_y y)/\sqrt{2})$, where j takes values I and III, $\alpha = \arcsin(\hbar v_F k_y / |\epsilon + \mu|)$ and $k_x(\epsilon) = \sqrt{[(\epsilon + \mu)/\hbar v_F]^2 - k_y^2}$. In region II, the presence of the ferromagnetic strip with a magnetization $\vec{m}_0 = m_0 \hat{y}$ leads to the additional term $H_{\text{induced}} = \int dx dy \mathcal{J} \theta(x) \theta(d-x) \psi^\dagger(\vec{x}) \sigma_y \psi(\vec{x})$, where $\mathcal{J} \sim m_0$ is the exchange field due to the presence of the strip [11], and $\theta(x)$ denotes the Heaviside step function. Note that H_{induced} may be thought as a vector potential term arising due to a fictitious magnetic field $\vec{B}_f = (\mathcal{J}/e v_F) \times [\delta(x) - \delta(d-x)] \hat{z}$. This analogy shows that our choice of the in-plane magnetization along \hat{y} is completely general; all gauge invariant quantities such as transmission are independent of the x component of \vec{m}_0 in the present geometry. Note that this effect is distinct from that due to a finite z component of \vec{m}_0 which provides a mass to the Dirac electrons. For a given m_0 , the precise magnitude of \mathcal{J} depends on the exchange coupling of the film and can be tuned, for soft ferromagnetic films, by an applied field [11]. The wave function for the Dirac fermions in region II moving along $\pm x$ in the presence of such an exchange field is given by $\psi_{\text{II}}^\pm = (1, \pm e^{\pm i\beta}) \exp(i(\pm k'_x x + k_y y)/\sqrt{2})$, where $\beta = \arcsin(\hbar v_F (k_y + M) / |\epsilon + \mu|)$, $M = \mathcal{J}/(\hbar v_F)$, and $k'_x(\epsilon) = \sqrt{[(\epsilon + \mu)/\hbar v_F]^2 - (k_y + M)^2}$. Note that beyond a critical $M_c = \pm 2|\epsilon + \mu|/(\hbar v_F)$ (and hence a critical $\mathcal{J}_c = \pm 2|\epsilon + \mu|$), k'_x becomes imaginary for all k_y , leading to spatially decaying modes in region II.

Let us now consider an electron incident on region II from the left with a transverse momentum k_y and energy ϵ . Taking into account reflection and transmission processes at $x = 0$ and $x = d$, the wave function of the electron can be written as $\psi_I = \psi_I^+ + r\psi_I^-$, $\psi_{\text{II}} = p\psi_{\text{II}}^+ + q\psi_{\text{II}}^-$, and

$\psi_{\text{III}} = t\psi_{\text{III}}^+$. Here r and t are the reflection and transmission amplitudes and p (q) denotes the amplitude of right (left) moving electrons in region II. Matching boundary conditions on ψ_I and ψ_{II} at $x = 0$ and ψ_{II} and ψ_{III} at $x = d$ leads to

$$\begin{aligned} 1 + r &= p + q, & e^{i\alpha} - r e^{-i\alpha} &= p e^{i\beta} - q e^{-i\beta}, \\ t e^{ik'_x d} &= p e^{ik'_x d} + q e^{-ik'_x d}, \\ t e^{i(k'_x d + \alpha)} &= p e^{i(k'_x d + \beta)} - q e^{-i(k'_x d + \beta)}. \end{aligned} \quad (2)$$

Solving for t from Eq. (2), one finally obtains the conductance $G = dI/dV = (G_0/2) \int_{-\pi/2}^{\pi/2} T \cos(\alpha) d\alpha$. Here $G_0 = \rho(eV) w e^2 / (\pi \hbar^2 v_F)$, $\rho(eV) = |(\mu + eV) / [2\pi(\hbar v_F)^2]|$ is the density of states (DOS) of the Dirac fermions and is a constant for $\mu \gg eV$, w is the sample width, and the transmission $T = |t|^2$ is given by

$$\begin{aligned} T &= \cos^2(\alpha) \cos^2(\beta) / [\cos^2(k'_x d) \cos^2(\alpha) \cos^2(\beta) \\ &+ \sin^2(k'_x d) (1 - \sin(\alpha) \sin(\beta))^2]. \end{aligned} \quad (3)$$

Equation (3) and the expression for G represent one of the main results of this work. We note that for a given α , T has an oscillatory (monotonically decaying) dependence on d provided k'_x is real (imaginary). Since k'_x depends, for a given α , on M , we find that one can switch from an oscillatory to a monotonically decaying d dependence of transmission in a given channel (labeled by k_y or equivalently α) by turning on a magnetic field which controls m_0 and hence M . Also since $-1 \leq \sin(\alpha) \leq 1$, we find that beyond a critical $M = M_c$, the transmission in all channels exhibits a monotonically decaying dependence on d . Consequently, for a thick enough junction one can tune G at fixed V and μ from a finite value to nearly zero by tuning M (i.e., m_0) through M_c . Thus such a junction may be used as a magnetic switch. These qualitatively different behaviors of the junction conductance G for M below and above M_c is demonstrated in Fig. 2 by plotting G as a function of effective barrier width $z = d|eV + \mu|/\hbar v_F$ for several representative values of $\hbar v_F M / |eV + \mu|$. Since T and hence G depends on M through the dimensionless parameter $\hbar v_F M / |eV + \mu|$, this effect can also be observed by varying the applied voltage V for a fixed μ , d , and M . In that case, for a reasonably large dimensionless barrier thickness $z_0 = d\mu/\hbar v_F$, G/G_0 becomes finite only beyond a critical voltage $|eV_c + \mu| = \hbar v_F M / 2$ as shown in Fig. 3 for several representative values of z_0 . This critical voltage V_c can be determined numerically by finding the lowest voltage for which G/G_0 exhibits a monotonic decay as a function of z_0 . The plot of eV_c/μ as a function of $\hbar v_F M / \mu$, shown in inset of Fig. 3, demonstrates the expected linear relationship between V_c and M . We note such a dependence of G on M or V requires the Dirac electrons to be spinors in physical spin space and is therefore impossible to achieve in graphene [12] or conventional 2D electron gas for which a proximate ferromagnetic film

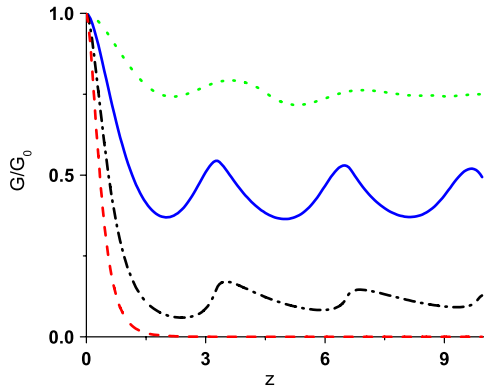


FIG. 2 (color online). Plot of tunneling conductance G/G_0 for a fixed V and μ as a function of the effective width $z = d|eV + \mu|/\hbar v_F$ for $\hbar v_F M/|eV + \mu| = 0.3$ (green dotted line), 0.7 (blue solid line), 1.3 (black dash-dotted line), and 2.1 (red dashed line). The value of the critical M is given by $\hbar v_F M/|eV + \mu| = 2$.

would only provide a Zeeman term for the electrons leaving G unaffected.

Next, we analyze the junction shown in the right panel of Fig. 1 where the region III below a ferromagnetic film is separated from region I by a potential barrier in region II. Such a barrier can be applied by changing the chemical region in region II either by a gate voltage V_0 or via doping [6]. In the rest of this work, we will analyze the problem in the thin barrier limit for which $V_0 \rightarrow \infty$ and $d \rightarrow 0$, keeping the dimensionless barrier strength $\chi = eV_0 d/(\hbar v_F)$ finite. The wave function of the Dirac fermions moving along $\pm x$ with a fixed momentum k_y and energy ϵ in this region is given by $\psi_{II}^{\pm} = (1, \pm e^{\pm i\gamma}) \exp(i(\pm k_x'' x + k_y y)/\sqrt{2})$, where $\gamma = \arcsin(\hbar v_F k_y/|\epsilon + eV_0 + \mu|)$ and $k_x''(\epsilon) = \sqrt{[(\epsilon + eV_0 + \mu)/\hbar v_F]^2 - k_y^2}$. The wave func-

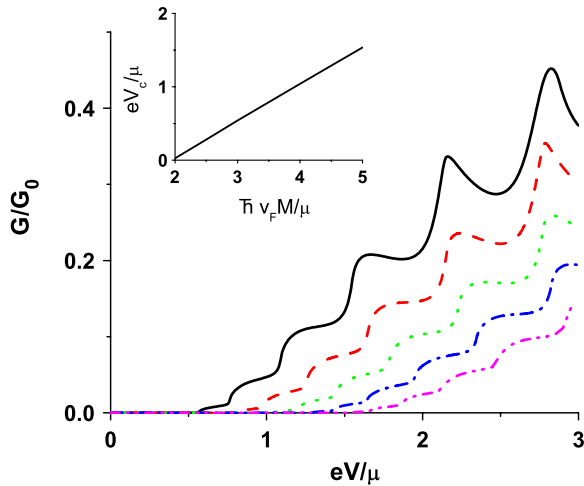


FIG. 3 (color online). Plot G/G_0 versus eV/μ for several representative values $\hbar v_F M/\mu$ ranging from 3 (leftmost black solid curve) to 5 (rightmost magenta dash-double dotted line) in steps of 0.5. The effective junction width $z_0 = 5$ for all plots. The inset shows a plot of eV_c/μ versus $\hbar v_F M/\mu$. See text for details.

tions in regions I and III are $\psi_I' = \psi_I$ and $\psi_{III}' = \psi_{II}$. Note that one can have a propagating solution in region III only if $|M| \leq |M_c|$.

The transmission problem for such a junction can be solved by a procedure similar to the one outlined above for the magnetic strip problem. For an electron approaching the barrier region from the left, we write down forms of the wave function in the three regions I, II, and III: $\psi_I' = \psi_I^+ + r_1 \psi_I^-$, $\psi_{II}' = p_1 \psi_{II}^+ + q_1 \psi_{II}^-$, and $\psi_{III}' = t_1 \psi_{II}^+$. As outlined earlier, one can then match boundary conditions at $x = 0$ and $x = d$, and obtain the transmission coefficient $T_1 = |t_1|^2 k_x'/k_x$ as

$$T_1 = 2 \cos(\beta) \cos(\alpha) / [1 + \cos(\beta - \alpha) - \cos^2(\chi) \{ \cos(\beta - \alpha) - \cos(\beta + \alpha) \}]. \quad (4)$$

Note that in the absence of the ferromagnetic film over region III, $\beta = \alpha$, and $T_1 \rightarrow T_1^0 = \cos^2(\alpha) / [1 - \cos^2(\chi) \times \sin^2(\alpha)]$. The expression for T_1^0 , reproduced here for the special case of $M = 0$, is well known from analogous studies in the context of graphene, and it exhibits both Klein paradox ($T_1^0 = 1$ for $\alpha = 0$) and transmission resonance ($T_1^0 = 1$ for $\chi = n\pi$) [13]. When $M \neq 0$, we find that the transmission for normal incidence ($k_y = 0$) does become independent of the barrier strength, but its magnitude deviates from unity: $T_1^{\text{normal}} = 2\sqrt{1 - (\hbar v_F M/|eV + \mu|)^2} / (1 + \sqrt{1 - (\hbar v_F M/|eV + \mu|)^2})$. The value of T_1^{normal} decreases monotonically from 1 for $M = 0$ to 0 for $|M| = |eV + \mu|/(\hbar v_F)$ and can thus be tuned by changing M (or V) for a fixed V (or M) and μ .

The conductance of such a junction is given by $G_1 = (G_0/2) \int_{-\alpha_1}^{\alpha_2} T_1 \cos(\alpha) d\alpha$, where $\alpha_{1,2}$ are determined from the solution of $\cos(\beta) = 0$ for a given M . A plot of G_1 as a function of $\hbar v_F M/|eV + \mu|$ and χ (for a fixed eV and μ) is shown in Fig. 4. We find that the amplitude of G_1 decreases monotonically as a function of $|M|$ reaching 0 at $M = M_c$ beyond which there are no propagating modes in region III. Also, as we increase M , the conductance

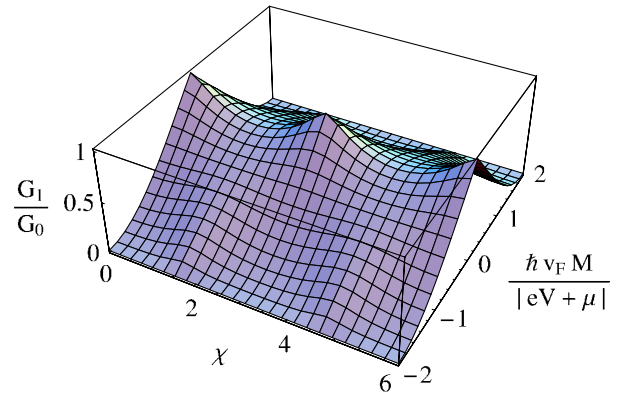


FIG. 4 (color online). Plot of tunneling conductance G_1/G_0 versus χ and M for a fixed applied voltage V and chemical potential μ . G_1 vanishes for $|M| \geq M_c = 2|eV + \mu|/\hbar v_F$.

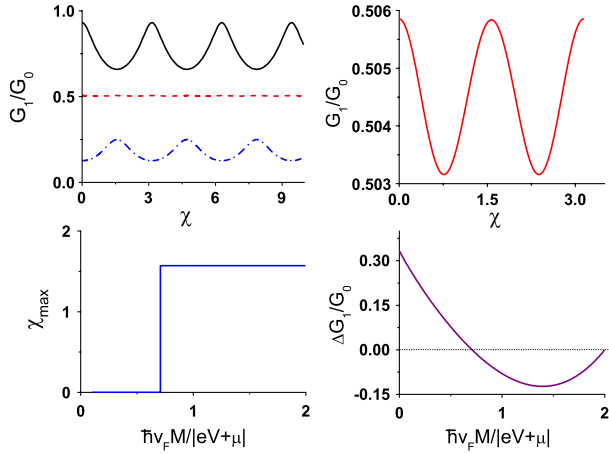


FIG. 5 (color online). Top left panel: Plot of G_1/G_0 versus χ for $\hbar v_F M/|eV + \mu| = 0.1$ (black solid line), 0.7075 (red dashed line), and 1.4 (blue dash-dotted line) for fixed V and μ . Top right panel: Plot of G_1/G_0 versus χ at $M = M^*$ showing the period halving. Bottom left panel: Plot of χ_{\max} versus $\hbar v_F M/|eV + \mu|$ showing conductance maxima positions. Bottom right panel: Plot of $\Delta G_1/G_0$ versus $\hbar v_F M/|eV + \mu|$ which crosses 0 at $M = M^*$. The dotted line is a guide to the eye.

maxima shifts from $\chi = n\pi$ to $\chi = (n + 1/2)\pi$ beyond a fixed value of $M^*(V) \approx \pm c_0 |eV + \mu|/(\hbar v_F)$ as shown in top left panel of Fig. 5. Numerically, we find $c_0 = 0.7075$. At $M = M^*$, $G_1(\chi = n\pi) = G_1(\chi = (n + 1/2)\pi)$, leading to a period halving of $G_1(\chi)$ from π to $\pi/2$. This is shown in top right panel of Fig. 5 where $G_1(M = M^*)$ is plotted as a function of χ . We note that near M^* , the amplitude of oscillation of G_1 as a function of χ becomes very small so that G_1 is almost independent of χ . In the bottom left panel of Fig. 5, we plot $\chi = \chi_{\max}$ (the value of χ at which the first conductance maxima occurs) as a function of $\hbar v_F M/|eV + \mu|$ which clearly demonstrates the shift. This is further highlighted by plotting $\Delta G_1 = G_1(\chi = 0) - G_1(\chi = \pi/2)$ as a function of $\hbar v_F M/|eV + \mu|$ in the bottom right panel of Fig. 5. ΔG_1 crosses zero at $M = M^* < M_c$ indicating the position of the period halving. Thus the position of the conductance maxima depends crucially on $\hbar v_F M/(eV + \mu)$ and can be tuned by changing either M or V .

The experimental verification of our results would involve preparation of junctions by depositing ferromagnetic films on the surface of a topological insulator. For the geometry shown in the left panel of Fig. 1, we propose measurement of G as a function of m_0 which can be tuned by an applied in-plane magnetic field [11]. We predict that depending on m_0 , G should demonstrate either a monotonically decreasing or an oscillatory behavior as a function of d . Another, probably more experimentally convenient, way to realize this effect would be to measure V_c of a junction of width d for several M and confirm that V_c varies linearly with M with a slope of $\hbar v_F/(2e)$, provided μ and d remain fixed. For the geometry depicted in the right panel of Fig. 1, one would, in addition, need to

create a barrier by tuning the chemical potential of an intermediate thin region of the sample as done earlier for graphene [12]. Here we propose measurement of G_1 as a function of V_0 (or equivalently χ) for several representative values of m_0 and a fixed V . We predict that the maxima of the tunneling conductance would shift from $\chi = n\pi$ to $\chi = (n + 1/2)\pi$ beyond a critical m_0 for a fixed V , or equivalently, below a critical V , for a fixed m_0 .

In conclusion, we have studied the transport of Dirac fermions on the surface of a topological insulator in the presence of proximate ferromagnetic films in two experimentally realizable geometries. Our study unravels novel features of the junction conductances which have no analog in either graphene or 2D Schrödinger electrons and can be verified in realistic experimental setups.

- [1] B. A. Bernevig, T. L. Hughes, and S.-C. Zhang, *Science* **314**, 1757 (2006); B. A. Bernevig and S.-C. Zhang, *Phys. Rev. Lett.* **96**, 106802 (2006).
- [2] M. Koenig *et al.*, *Science* **318**, 766 (2007); D. Hsieh *et al.*, *Nature (London)* **452**, 970 (2008).
- [3] C. L. Kane and E. J. Mele, *Phys. Rev. Lett.* **95**, 226801 (2005); **95**, 146802 (2005).
- [4] L. Fu, C. L. Kane, and E. J. Mele, *Phys. Rev. Lett.* **98**, 106803 (2007); R. Roy, *Phys. Rev. B* **79**, 195322 (2009); J. E. Moore and L. Balents, *Phys. Rev. B* **75**, 121306(R) (2007).
- [5] X. L. Qi, T. L. Hughes, and S. C. Zhang, *Phys. Rev. B* **78**, 195424 (2008); H. Zhang *et al.*, *Nature Phys.* **5**, 438 (2009).
- [6] Y. Xia *et al.*, *Nature Phys.* **5**, 398 (2009); arXiv:0907.3089 (unpublished).
- [7] Y. L. Chen *et al.*, *Science* **325**, 178 (2009); T. Zhang *et al.*, arXiv:0908.4136v3 (unpublished).
- [8] D. Hsieh *et al.*, *Nature (London)* **460**, 1101 (2009); P. Roushan *et al.*, *Nature (London)* **460**, 1106 (2009); D. Hsieh *et al.*, *Science* **323**, 919 (2009).
- [9] L. Fu and C. L. Kane, *Phys. Rev. Lett.* **100**, 096407 (2008).
- [10] A. R. Akhmerov, J. Nilsson, and C. W. J. Beenakker, *Phys. Rev. Lett.* **102**, 216404 (2009); Y. Tanaka, T. Yokoyama, and N. Nagaosa, *Phys. Rev. Lett.* **103**, 107002 (2009).
- [11] T. Yokoyama, Y. Tanaka, and N. Nagaosa, arXiv:0907.2810v2 (unpublished).
- [12] A. Castro Neto *et al.*, *Rev. Mod. Phys.* **81**, 109 (2009); C. W. J. Beenakker, *Rev. Mod. Phys.* **80**, 1337 (2008).
- [13] M. I. Katsnelson, K. S. Novoselov, and A. K. Geim, *Nature Phys.* **2**, 620 (2006); C. W. J. Beenakker, *Phys. Rev. Lett.* **97**, 067007 (2006); S. Bhattacharjee and K. Sengupta, *Phys. Rev. Lett.* **97**, 217001 (2006).
- [14] Analogous situations may arise for graphene electrons in the presence of suitable gate voltages, but not ferromagnetic films; see M. M. Fogler, F. Guinea, and M. I. Katsnelson, *Phys. Rev. Lett.* **101**, 226804 (2008).
- [15] The orbital effect of magnetic field along z in a multiple-barrier geometry may also reduce transmission in single and bilayer graphene. However, this property does not rely on Dirac nature of graphene electrons. See M. R. Masir *et al.*, *Appl. Phys. Lett.* **93**, 242103 (2008).